

Achievement of Current Pulses of High Amplitude Using a Voltage Pulse Generator

Ion Pătru, Marcel Nicola, Camelia Marinescu, Laurențiu Vlădoi and Maria Cristina Nițu

National Institute for Research Development and Testing in Electrical Engineering - ICMET Craiova/
Research and Development Division, Craiova, Romania

ipatru@icmet.ro, marcel_nicola@yahoo.com, micro@icmet.ro, vladoilaurentiu@icmet.ro, cristinanitu@icmet.ro

Abstract - This paper presents a comprehensive project aiming to achieve high amplitude current impulses using a high voltage generator (GIT) as a power supply. To obtain impulse currents with GIT, a wide range of simulations has been carried out to obtain the optimal parameters of the current impulse. LC delay cells were introduced in the test system circuit in order to increase the duration of the current impulse. A current impulse generator (GIC) circuit has been developed to meet the standards in force. This system has enabled new test methods to be developed and improved equipment developed. The development of this project allowed current impulses to be obtained with minimum costs. The methods and procedures used can be used to expand research fields by using current impulses to determine the dynamic and thermal stability of electrotechnical and electro-energetic equipment as well as the functional stability of electronic devices in electromagnetic disturbed environments.

Cuvinte cheie: impuls de curent, generator impuls de tensiune, impuls de trasnet, curenti mari.

Keywords: impulse current, impulse voltage generator, lightning impulse, high currents.

I. INTRODUCTION

The safe operating life of electrical equipment is ensured by achieving a construction which has taken into account the possible dielectric, thermal and mechanical stress which they may undergo, by carrying out proper maintenance, equipping them with means of signalling, by monitoring the critical internal parameters and by providing fast intervention in case of failure.

The reliable operating life of electrical equipment is provided by a setup which considers the possible dielectric, thermal and mechanical stress to which it may be subjected [1-3], by providing proper maintenance, means of signalling, internal critical parameter monitoring and rapid intervention in case of defects.

Extreme dielectric and mechanical stress occurs in the case of transient regimes such as: surges caused by the lightning impulse [4-6] no-load connection and two or three-phase short-circuit.

The study of transient phenomena and the propagation of voltage waves in both electrical networks and electrical equipment allows information to be obtained on the insulation stress level, the factors influencing the shape and amplitude of surges and even on the effectiveness of the protection schemes adopted [7], [8].

For these reasons, the testing of electrical and power equipment is strictly necessary [9], both to ensure their constructive and operating quality, throughout their operating life, and to meet the necessary conditions for launching product (equipment) manufacturing.

The electrical equipment testing is carried out in specialized laboratories, equipped with suitable installations and stations for verifying the quality of execution of the equipment concerned, as well as for certification that the achieved equipment will withstand throughout its operating life, provided that the operating conditions are met. At the same time, the testing also aims, in case the equipment under test does not withstand the test run, to reveal and locate the defects, since some of these are rather difficult to track, and the designer and the manufacturer need this information. Since unfortunately there are more than a single method of detecting these defects, a test method, with the proper installation being applied for each type of defect, it follows that these laboratories are very complex, with a multitude of testing facilities, with standardized testing methodologies and equipment [10-19]

The destructive high voltage insulation tests are performed in special high-voltage laboratories equipped with suitable technological systems allowing the determination of critical parameters of the equipment under test.

The most important equipment of high voltage laboratories are the a.c. d.c. and impulse high voltage sources, as well as the appropriate measurement equipment [20-22]. For high and very high voltage electrical equipment, the transportation to these fixed laboratories is particularly cumbersome, which is why high performance portable testing equipment was designed.

High voltage laboratories include equipment intended for the generation and measurement of: power-frequency a.c. high voltage, lightning impulse high voltage, impulse switching high voltage, d.c. high voltage, impulse current, as well as mixed impulse current and a.c. voltage equipment.

The thermal characteristics of the test equipment are determined by the levels of the test voltages to be achieved which in turn are determined based on the insulation coordination principles. The test equipment must ensure the prescribed parameters and the electrical quantities they produce. In addition, the test installations are equipped with measuring schemes which must ensure the conversion of high voltages to values suitable for measurements or recording.

The following chapters present the development of a current impulse testing system for high voltage equipment by using existing equipment. An impulse current-shaping circuit [23-24] will be achieved to meet the standards in force. Its power supply will be provided by the existing high voltage impulse generator [25-27] and the measuring elements used will be the high voltage divider, the shunt circuits and the rapid signal recording systems.

II. VOLTAGE GENERATOR

The testing carried out on the electrical and power equipment is strictly necessary both to ensure their design and operation quality, and to fulfill the requirements for launching the manufacturing of a new product.

The impulse voltage generator is intended to generate impulse voltage waves of certain shapes and amplitudes, which are generally standardized.

The shape and parameters of the lightning impulse voltage.

The shape of these voltages is generally aperiodic impulse, initially with a rapid increase (front) up to the peak value, followed by a slower decrease (back), but whose durations may vary within relatively wide limits. Following laboratory studies on the behaviour of insulation to such stress, a standard shape of the lightning impulse voltage (ITT) has been defined, which is characterized by the conventional durations of the front ($1.2 \mu\text{s}$) and the semi-amplitude ($50 \mu\text{s}$) - see Fig. 1.

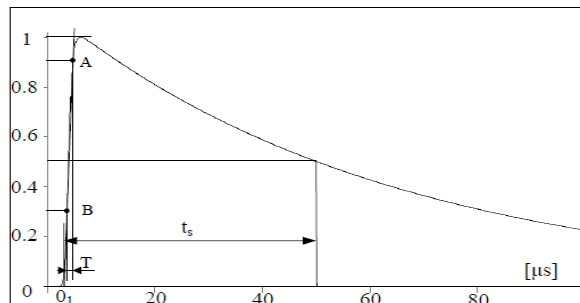


Fig. 1. Standard impulse waveforms.

The lightning impulse voltage (ITT) is full if not interrupted by a disruptive discharge. If the impulse applied to the insulation generates an electric discharge, the voltage drops to zero at the moment of the discharge, respectively the impulse is chopped. The chopping can occur on the front, the front or the back of the impulse.

The generation of the lightning impulse voltages

To generate the voltage waveforms shown in Fig. 1, impulse voltage generators are used. The most commonly used schematic diagram of such a generator has the configuration shown in Fig. 2.

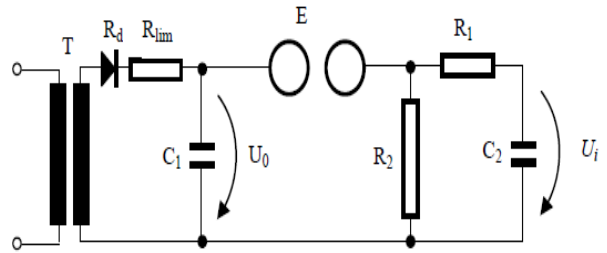


Fig. 2. Schematic diagram for the generation of the aperiodic impulse voltage.

The impulse capacitor C_1 is charged from a rectified high voltage source, consisting of the power transformer T and the rectifier R_d . When the voltage at its terminals reaches the value U_0 , equal to the breakdown voltage of E , then the capacitor starts.

The impulse voltage U_i at the C_2 load capacitor terminals has a double exponential shape, expressed by the relation:

$$U_i(t) = \eta U_0 \left(e^{\frac{-t}{T_1}} - e^{\frac{-t}{T_2}} \right) \quad (1)$$

The dimensionless parameter η and the time constants T_1 and T_2 depend on the structure of the diagram and the sizes of its components.

In the case of the diagram shown in Fig. 2, the impulse parameters (durations t_f and t_s) and duty factor can be calculated by using the following approximate formulas:

$$t_f = 2.96 R_1 \frac{C_1 C_2}{C_1 + C_2}; \quad (2)$$

$$t_s = 0.73 R_2 (C_1 + C_2)$$

III. IMPULSE CURRENT GENERATOR

The assessment of the surge behavior of electric insulating structures caused by lightning discharges requires the generation in the laboratory of a voltage whose waveform should correspond to the records obtained experimentally, during storms with such discharges. The waveform of these voltages is a generally aperiodic impulse, with an initial rapid increase to peak, followed by a slower decrease, but whose durations may vary within relatively wide limits. The studies carried out over time allowed a standard lightning impulse voltage (ITT) waveform to be defined, characterized by the conventional $1.2 \mu\text{s}$ front time and the $50 \mu\text{s}$ time to half value.

The aim of this study is to achieve an impulse current test system for high voltage equipment by using an impulse voltage generator.

An impulse current-shaping circuit was achieved to meet the standards in force, starting from the fact that the repetitive diagram for an impulse current generator is essentially the same as for an impulse voltage generator, except that in this case the capacitor discharge in a RL circuit is considered.

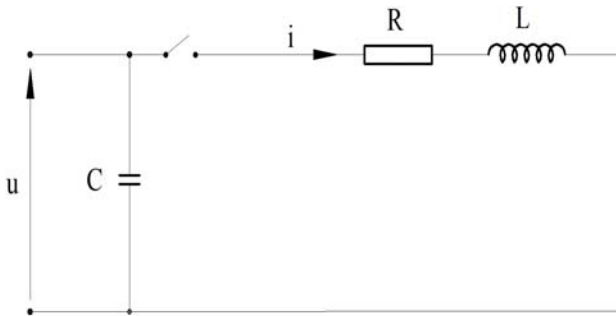


Fig. 3. The repetitive diagram for the impulse current generator is of series RLC type.

The repetitive diagram for the impulse current generator is of the series RLC type (see Fig. 1), and the ideal-case sizing of the impulse-shaping circuit is achieved, where the internal resistance of the impulse energy storage capacities, as well as the internal resistance of object under test are considered negligible.

The purpose of the impulse current generator is to be able to supply high and very high current impulses. The peak power of such a generator can reach approximately 200 kW, at impulse currents with value up to the 100kA peak and peak voltages applied up to 200kV [8], [10].

The operating equations for the impulse current generator assimilated to an RLC circuit are [8], [26]:

- for linear resistance:

$$L \frac{di(t)}{dt} + Ri(t) + \frac{1}{C} \int i(t) dt = U \quad (3)$$

- for nonlinear resistance:

$$L \frac{di(t)}{dt} + Ri(t) + \frac{1}{C} \int i(t) dt + ki(t)^a = U \quad (4)$$

where $U_r = ki^a$ represents the voltage across nonlinear resistance, equation (4) defines the impulse current generator specific application for testing metal oxide varistors or arresters.

From equation (3) after differentiation and rearrangement, we obtain a homogeneous equation:

$$\frac{d^2i(t)}{dt^2} = -\frac{R}{L} \frac{di(t)}{dt} - \frac{1}{LC} i(t) \quad (5)$$

This equation has 3 types of solutions corresponding to the 3 main impulse discharge conditions, determined by the value of the term $R^2 - 4L/C$.

In practice, the critical damped regime is excluded because the equality $R^2 = 4L/C$ will not be possible, therefore we will have the following [2] equivalents:

- overdamped regime = aperiodic regime, when $R^2 - 4L/C > 0$;
- underdamped regime = damped harmonic regime, when $R^2 - 4L/C < 0$.

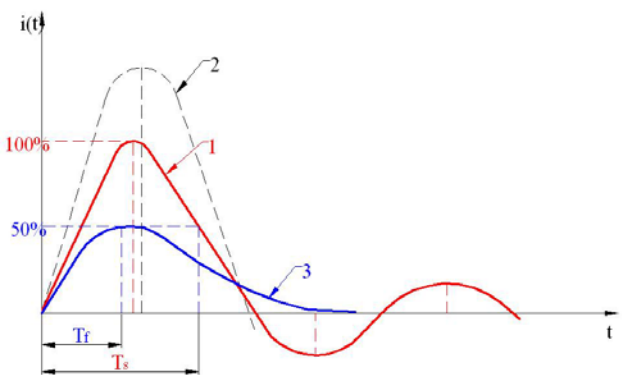


Fig. 4. Standard impulse waveforms.

where: 1- damped harmonic regime;

2- undamped harmonic regime;

3- aperiodic regime;

T_f – front time;

T_s – time to half value.

The three characteristic regimes of the RLC circuit are represented in Fig. 4:

The impulse voltage and impulse current measurement, assessment and analysis system must comply with the standards [11-17].

A solution with damped oscillation waveform is obtained on condition that [28-30]:

$$\frac{R}{2} < \sqrt{\frac{L}{C}} \quad (6)$$

In this case, the solution of the equation has the following form [28-30]:

$$i = \frac{U}{\omega L} e^{-\alpha t} \sin \omega t \quad (7)$$

where:

$\alpha = \frac{R}{2L}$ represents the circuit damping factor

$\omega = \sqrt{\frac{1}{LC} - \frac{R^2}{4L^2}}$ it is the pulse wave oscillating

The rise time of the impulse current amplitude from zero to the first peak is the front time:

$$T_1 = T_f = \frac{1}{\alpha} \tan \left(\frac{\omega}{\alpha} \right) \quad (8)$$

To simplify the calculation, the following approximation is made:

$$T_1 \approx \frac{1}{\alpha} \quad (9)$$

For small values of ω according to [28-30], T_2 is given by the equation

$$T_2 = 2.678 \cdot T_1 = 2.678 \cdot \frac{1}{\alpha} \quad (10)$$

After the parameters are determined theoretically, circuit elements sizing is carried out next. As per Fig. 3 we consider a total capacitance $C=10\mu F$ for the capacitive elements. Their charge voltage is from zero to peak working voltage. In the case of the lightning impulse voltage generator, it may reach 200kV. For a 5Ω total resistance in the circuit, we will determine the parameters of the other circuit elements. Their values will be

corrected based on experimentation. $L > \frac{R^2 C}{4}$ results from relation (6), and by replacing the values determined, we obtain:

$L=75\mu H$, and $\omega = 15 \cdot 10^3 \text{ rad/s}$.

For the circuit in Fig. 3, in addition to the value of the circuit elements, we have the front time $T_1=28\mu s$ and back time $T_2=75\mu s$ determined.

According to the approximation calculations, the circuit elements are sized for an impulse with $T_1/T_2=8/20\mu s$ waveform.

In order to achieve a pulse current generator starting from an impulse voltage generator (GIT) operating scheme [18], [23], [26], LC delay impulse cells must be introduced into the circuit

For the Coil sized are imposed the following conditions: $L=75\mu\text{H}$; $I_{\max}=20\text{kA}$; $U_{\max}=100\text{kV}$ and $8/20\mu\text{s}$ impulse current. A cylindrical coil without core is adopted in one layer [1-3], realized by copper profile conductor CuE29 $4\times10\text{ mm}^3$.

IV.DETERMINATION OF IMPULSE CURRENT GENERATOR PARAMETERS BY SIMULATION

The determination of the parameters of the current impulse shaping circuit components is carried out based on the GIT parameters [26]. It consists of 14 floors with 8 impulse capacitors on each floor. The nominal value of the capacitor parameters is of 72nF/300kV. The connection with 14 floors in parallel is adopted, therefore the maximum equivalent capacity is 8064nF.

To generate an impulse current without using any impulse-shaping circuits, and based only on the internal parameters of the impulse voltage generator, the circuit diagram which includes only the parameters of the impulse voltage generator in Fig. 3 is adopted.

The diagram used for simulation is shown in Fig. 5 and its parameters are prescribed for: $C_i=5\mu F$, $R_p=1000\Omega$, $R_f=30\Omega$, $L=1mH$, $C_s=100pF$, $R_s=10m\Omega$, $L_s=10\mu H$.

Fig. 6 presents the voltage $u(t)$ and current $i(t)$ waveforms obtained by simulation.

By modifying the prescribed parameters $C_i = 10\mu F$, $R_p = 2000\Omega$, $R_f = 1\Omega$, $L = 1mH$, $C_s = 50pF$, $R_s = 10\mu\Omega$, $L_s = 10\mu H$, a new impulse current waveform is obtained (Fig. 7).

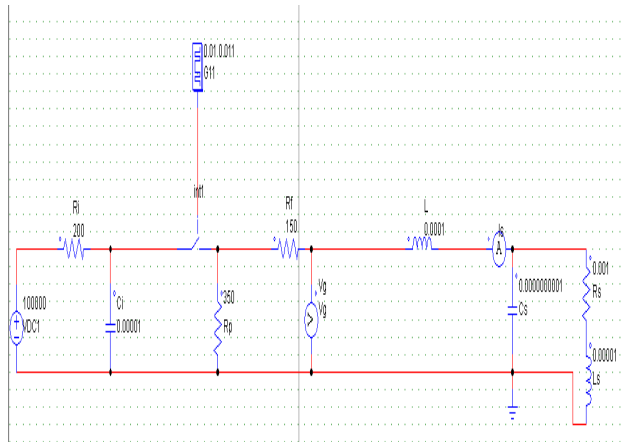


Fig. 5. The simple circuit diagram of the impulse current generator (GIC).

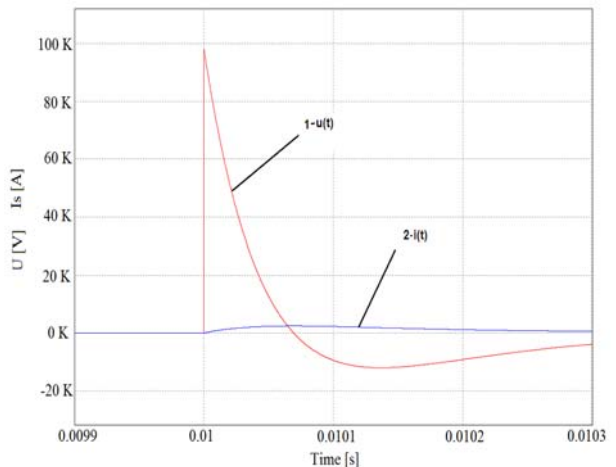


Fig. 6. Impulse voltage ($u(t)$) and impulse current ($i(t)$) waveforms.

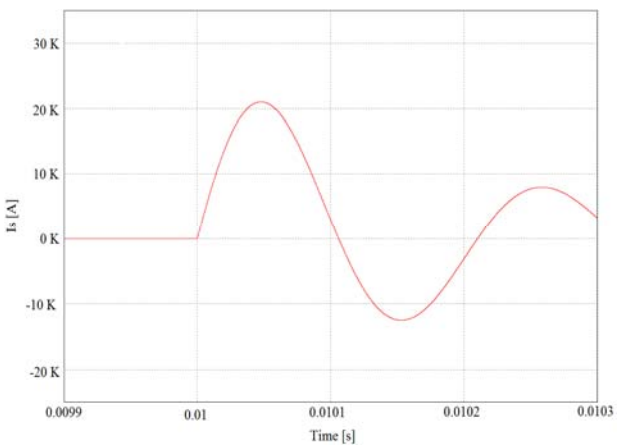


Fig. 7. Impulse current waveform.

To extend the T_2 of the current wave, a current impulse-shaping circuit diagram was modelled/simulated, which has a LC cell Fig. 8.

For the prescribed parameters of the circuit elements: $C_i=10\mu F$, $R_p=150\Omega$, $R_f=15\Omega$, $L=0.1mH$, $C_s=100pF$, $R_s=1m\Omega$, $L_s=10\mu H$, $L_c=0.1mH$, $C_c=1\mu F$, the following

impulse current waveforms were obtained by simulation (Fig. 9).

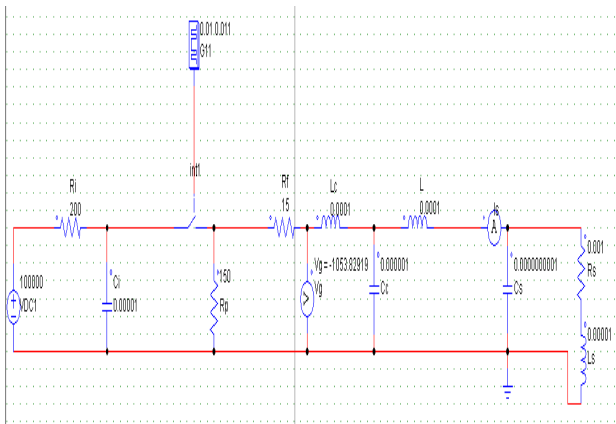


Fig. 8. The impulse current generator circuit diagram with a LC delay cell.

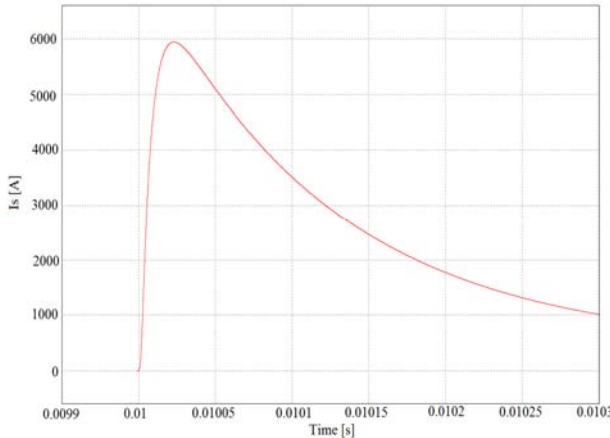


Fig. 9. Impulse current waveform with a LC delay cell.

To extend the T_2 of the current wave, a current impulse-shaping circuit diagram was modeled/simulated, which has three LC cell Fig. 10.

By modifying the prescribed parameters $C_i = 10\mu F$, $R_p = 1500\Omega$, $R_f = 15\Omega$, $L = 0.1mH$, $C_s = 100pF$, $R_s = 0.1m\Omega$, $L_s = 10\mu H$; $L_c = 0.01mH$, $C_c = 0.01\mu F$, a new impulse current waveform is obtained (Fig. 11).

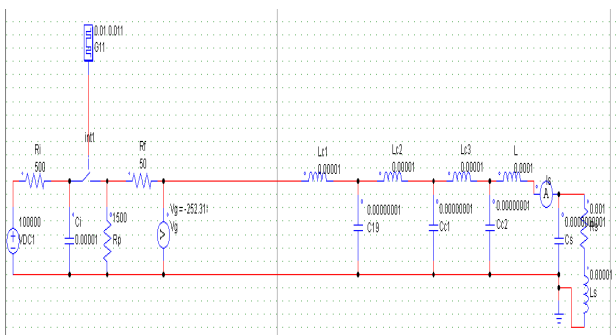


Fig. 10. The impulse current generator circuit diagram with 3 LC delay cell.

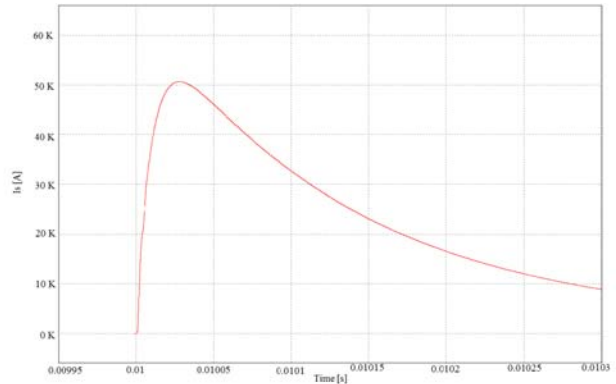


Fig. 11. Impulse current waveform with 3 LC delay cell.

To emphasize the influence of the delay cells on the impulse current, a circuit diagram in which six such cells were included in the current impulse-shaping circuit was analyzed, with the following prescribed parameters: $C_i = 10\mu F$, $R_p = 1500\Omega$, $R_f = 1\Omega$, $L = 0.1mH$, $C_s = 100pF$, $R_s = 0.1m\Omega$, $L_s = 10\mu H$; $L_c = 0.01mH$, $C_c = 0.01\mu F$ (Fig. 12).

By simulation, in case of adopting the circuit diagram shown in Fig. 12, the waveform for the impulse current is shown in Fig. 13.

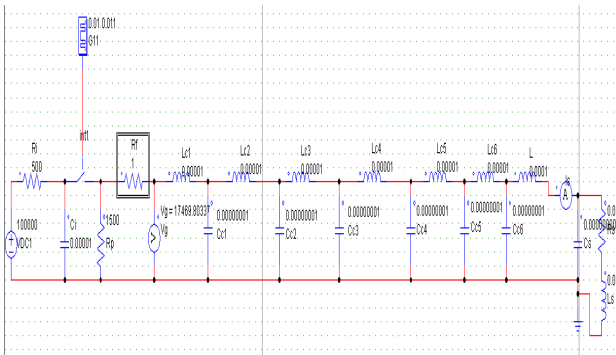


Fig. 12. Circuit diagram achieved by adding 6 LC delay cells in the current impulse-shaping circuit.

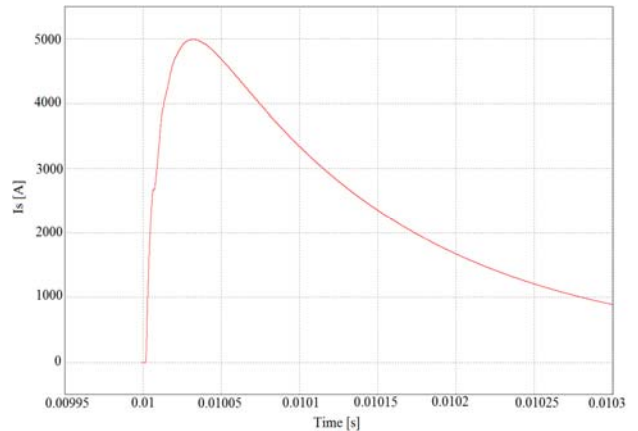


Fig. 13. Impulse current waveform with 6 LC delay cell.

V. TEST RESULTS

The figure 14 presents the achieved construction of the power unit with variable voltage and frequency as well as modules included herein.



Fig. 14. The achieved construction of the power unit with variable voltage and frequency.

The system used to carry out the experiments consists of:

- adjustable voltage static converter;
 - high voltage lightning impulse generator;
 - high voltage circuit elements up to 300kV: capacitors, resistors, inductive elements.

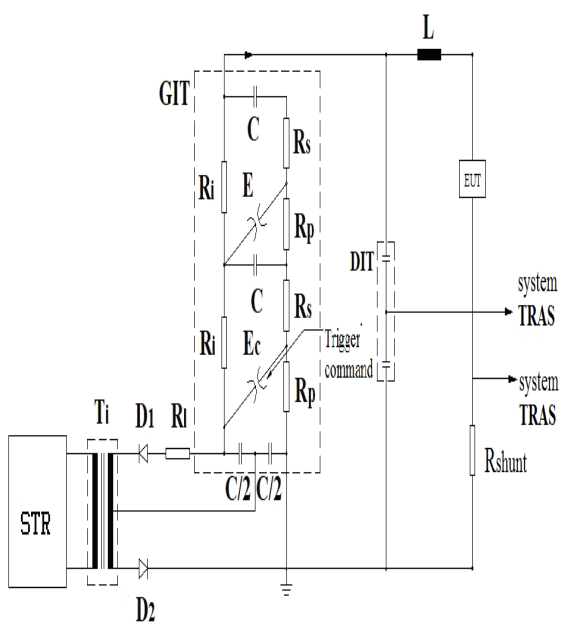


Fig. 15. Experimental diagram.

The diagram presented in figure 15 was used during the experiments, where:

STR – Variable voltage source; Ti – High-voltage step-up transformer; D1; D2 – High-voltage rectification systems; RI – Resistor to load current limitation; Rs –

Discharge resistors in series with the test circuit; R_p - Discharge resistors in parallel with the test circuit; R_i - Resistor for capacitor charging; C - Shock capacities of the voltage pulse generator (GIT); GIT - Impulse voltage generator assembly; DIT - high-voltage divider; L - inductance consisting of coils for the formation of the impulse current; EUT - object under test; R_{shunt} - resistance for current measurement; EC - discharger with impulse trigger control; E - discharger for capacity separation.

The measuring and recording element used for current and voltage was a **TRAS** type rapid signal recording system.

To validate the results obtained by simulation, the following impulse voltage test circuits were achieved, with the next parameters:

- $U_p=26\text{kV}$, $1/4\mu\text{s}$; $R_s=0.001\Omega$ and $L=100\mu\text{H}$, $I_p=57\text{kA}$; $T_1=8\mu\text{s}$ and $T_2=25\mu\text{s}$ (Fig. 16);

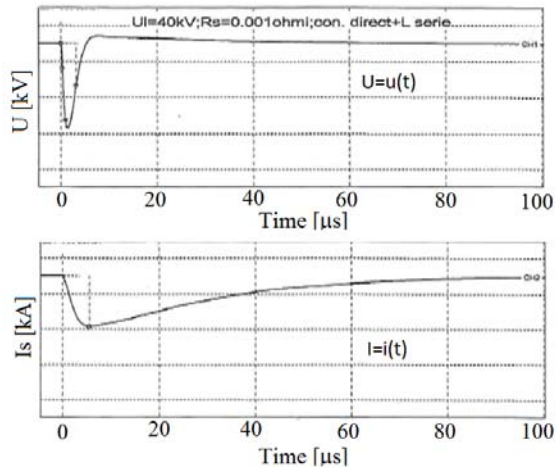


Fig. 16. Impulse voltage $u(t)$ and impulse current $i(t)$ waveforms.

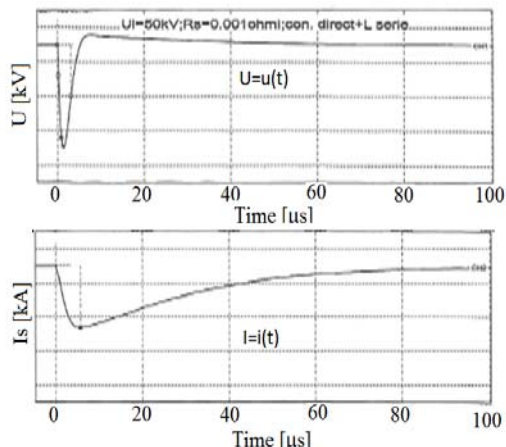


Fig. 17. Impulse voltage $u(t)$ and impulse current $i(t)$ waveforms.

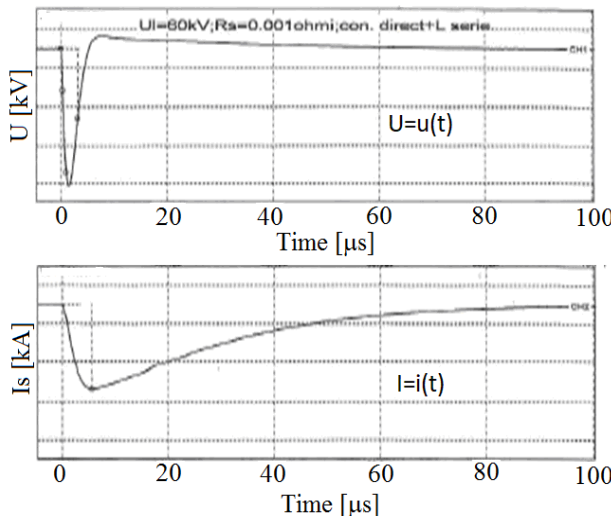


Fig. 18. Impulse voltage $u(t)$ and impulse current $i(t)$ waveforms.

It is noted that the circuit can be used for obtaining impulse currents which can be used for research in relation to voltage-dependent variable-resistance arresters.

For measuring the voltage pulse a capacitive divider was used with very low response time capable of measuring voltages with $1000\text{kV}/\mu\text{s}$ rise time.

To measure the impulse current, a capacitive divider was used, with very low response time, capable of measuring voltages with $100\text{kA}/\mu\text{s}$ rise time.

To measure the impulse current, shunts with very low inductances and parasitic capacitances were used, so that the current increases of over $100\text{kA}/\mu\text{s}$ can be measured.

As a result of the tests, in order to obtain a $8/20\ \mu\text{s}$ current in the allowed tolerances according to the proposed ones and taking into account the internal parameters of the generator, the following results are obtained:

- the impulse voltage is applied directly to the test object (with no separation). Its optimum form is $1/3\mu\text{s}$;

- the series inductance introduced into the circuit should be about $100\mu\text{H}$ (the value of the circuit self-inductance is also added);

- the total series resistances (including those of the impulse voltage generator) should be 1Ω max.;

- a shunt with $R=0.001\ \Omega$ resistance was used for the measurement.

There are cases where, due to the nature of load of the test object (inductive, capacitive or resistive), the form of the impulse current varies greatly for the same values and forms of the impulse voltage applied.

In the case of an inductive load, if there are no resistive elements for fast damping of impulse (aperiodic form), there are oscillations due to the capacitance of the high voltage divisional and the inductance of the circuit (periodic oscillation), which can be more or less damped.

If, in the case of the circuit, there is insulating space (discharge in air), the circuit is highly damped due to the predominantly resistive nature of the electrical discharge in air. In this case there are only high-frequency oscillations (in the order of MHz) due to the disturbing capacitances and inductances (resonant own resonance frequencies) at the moment of ionized space breakdown.

VI.CONCLUSIONS

In this paper studies were conducted on the impulse current and voltage generation systems used in the development and testing of electrotechnical equipment.

In order to use the impulse voltage generator to generate impulse currents, various circuit diagrams have been studied and the parameters of the circuit elements have been determined based on numerical simulations, with a view to obtaining the necessary impulse current forms.

The results obtained with this study confirm that various impulse current values and forms can be obtained by executing certain circuit elements (coils) and by using the proper capacitances.

The limits of using the high voltage impulse generator to generate high-energy impulse current have been determined.

The methods and procedures applied can be used to expand the research areas by using the high-energy impulse currents: the dynamic and thermal stabilities of electrotechnical and power equipment, research on the operating stability of electronic devices in environments with high electromagnetic interference.

ACKNOWLEDGMENT

The paper was developed with funds from the Ministry of Research and Innovation as part of the NUCLEU Program: PN 16 15 01 04 and PN 19 38 01 03.

Contribution of authors:

First author – 40%

First coauthor – 15%

Second coauthor – 15%

Third coauthor – 15%

Fourth coauthor – 15%

Received on July 17, 2019

Editorial Approval on November 15, 2019

REFERENCES

- [1] C. I. Nicola, M. Nicola, I. Pătru, M. C. Nițu, V. Voicu, and S. Popescu, "Application software for reactor sizing calculation," *The International Conference on Hydraulics and Pneumatics HERVEX – 23nd edition*, Băile Govora, Romania, 2017, pp. 264-273.
- [2] P. L. Kalantarov and L. A. Teitlin, *Calculation of inductances*, Technical publishing house, 1958.
- [3] [1] C. I. Nicola, M. Nicola, I. Pătru, V. Voicu, and S. Popescu, "Reactor Sizing Calculation using Virtual Instrumentation," in *International Journal of Engineering Technology and Scientific Innovation (IJETSI)*, vol. 3, no. 4, pp. 140-159, June 2018.
- [4] B. Wang, Z. Fu, and N. Yan, "Design of multi-component impulse current generator for practical lightning current simulation," *International Conference on Lightning Protection (ICLP)*, Shanghai, China, 2014, pp. 278-282.
- [5] M. C. Nițu, C. I. Nicola, D. Popa, V. Voicu, and M. Dută, "Lightning impulse type overvoltage transmitted between the windings of the transformer," *International Symposium on Fundamentals of Electrical Engineering (ISFEE)*, Bucharest, Romania, 2016, pp. 1-5.
- [6] M. C. Nițu and M. D. Dută, "Calculation of Surges Transmitted Between Transformer Windings Using the Coupled Circuit Model," *International Conference on Applied and Theoretical Electricity (ICATE)*, Craiova, Romania. 2018, pp. 1-6.

- [7] EN 50164-2, Lightning protection system components – Requirements for conductors and earth electrodes.
- [8] G. Dradan, *High voltage technique. vol. I*, Technical Publishing, 1996.
- [9] Wolfgang Hauschild Eberhard Lemke, *High Voltage Test and Measuring Techniques*, Springer, Verlag Berlin Heidelberg, 2014.
- [10] ***www.highvolt.de – SR-3-40-5.pdf.
- [11] IEC 60076-22-1:2019 - Power transformers - Part 22-1: Power transformer and reactor fittings – Protective devices.
- [12] IEC 61083-1:2001 - Instruments and software used for measurement in high-voltage impulse tests - Part 1: Requirements for instruments
- [13] IEC 61083-2:2013 - Instruments and software used for measurement in high-voltage and high-current tests - Part 2: Requirements for software for tests with impulse voltages and currents.
- [14] IEC 60060-1:2010 - High-voltage test techniques - Part 1: General definitions and test requirements.
- [15] IEC 60060-2:2010 - High-voltage test techniques - Part 2: Measuring systems.
- [16] IEC 60099-4:2014 - Surge arresters - Part 4: Metal-oxide surge arresters without gaps for a.c. systems.
- [17] IEC 60230:2018 - Impulse tests on cables and their accessories.
- [18] ***www.haefely-hipotronics.com – LL_GC_257_151204.pdf; LL_SSG.pdf.
- [19] *** NFC 17102 english version 15-11-2011.pdf.
- [20] S. Shalamov, “Current Measuring Shunts for Impulse Current Test According to IEC 62305–2010,” *9th International Conference on Ultrawideband and Ultrashort Impulse Signals (UWBUSIS)*, Odessa, Ukraine , 2018, pp. 127-130..
- [21] L. Frolek and J. Souc, “Measurement of Current-Voltage Curves of Superconducting Tapes by Means of Quasi Trapezoidal Current Impulses,” in *IEEE Transactions on Applied Superconductivity*, vol. 19, no. 3, pp. 3581-3584, June 2009.
- [22] Y. Yuan, F. Jianqiang, J. Ning, J. Zhuanzhuan, and L. He, “Study on calibration of impulse current measuring system,” *13th IEEE International Conference on Electronic Measurement & Instruments (ICEMI)*, Yangzhou, China, 2017, pp. 415-420.
- [23] M. Modrusan, Normalized calculation of impulse current circuits for given impulse current – HAEFELY Translated from Bulletin ASE. Bd. 67(1976). 22.
- [24] R. Ferraz, S. Oliveira, A. Silva, J. Nerys, A. Alves, and W. Calixto, “Construction of an impulse current generator prototype applied in electrical grounding systems,” *CHILEAN Conference on Electrical, Electronics Engineering, Information and Communication Technologies (CHILECON)*, Santiago, Chile, 2015, pp. 649-653.
- [25] Karel Veisheipl, “Simulation of the high voltage impulse generator,” *International Scientific Conference on Electric Power Engineering (EPE)*, pp.1-5, Prague, Czech Republic, 2016.
- [26] J. Hlavacek and M. Knenicky, “Very fast high voltage impulse generator,” *19th International Scientific Conference on Electric Power Engineering (EPE)*, Brno, Czech Republic, 2018, pp. 1-4.
- [27] I. Pătru, M. Nicola, C. Marinescu, L. Vlădoi, and M. C. Nișu, “Applications of Voltage Pulse Generator to Achieve Current Pulses of High Amplitude,” *International Conference on Electro-mechanical and Energy Systems (SIELMEN)*, Chisinau, Moldova, 2019, pp. 1-6.
- [28] Gh. Hortopan, *Electrical appliances*, Didactic and pedagogical publishing house, Bucuresti, 1984.
- [29] Ye. Trotsenko, V. Brzhezitsky, and I. Masluchenko, “Analytical representation of switching current impulses or study of metal-oxide surge arrester models,” in *Technology audit and Production Reserves*, vol. 5, no. 1(37), pp. 24-30, December 2017.
- [30] N. H. Halim, A. Azmi, Y. Yahya, F. Abdullah, M. Othman, and M. S. Laili, “Development of a small scale standard lightning impulse current generator,” *5th International Power Engineering and Optimization Conference*, Shah Alam, Selangor, Malaysia, 2011, pp. 426-431.